CONDENSED MATTER PHYSICS

Direct visualization of coexisting channels of interaction in CeSb

Sooyoung Jang[1,2,3]*, Robert Kealhofer[2,3], Caolan John[2,3], Spencer Doyle[2,3], Ji-Sook Hong[4], Ji Hoon Shim[4], Q. Si[5], O. Erten[6], Jonathan D. Denlinger[1]*, James. G. Analytis[2,3]*

Our understanding of correlated electron systems is vexed by the complexity of their interactions. Heavy fermion compounds are archetypal examples of this physics, leading to exotic properties that weave magnetism, superconductivity and strange metal behavior together. The Kondo semimetal CeSb is an unusual example where different channels of interaction not only coexist, but have coincident physical signatures, leading to decades of debate about the microscopic picture describing the interactions between the f moments and the itinerant electron sea. Using angle-resolved photoemission spectroscopy, we resonantly enhance the response of the Ce f electrons across the magnetic transitions of CeSb and find there are two distinct modes of interaction that are simultaneously active, but on different kinds of carriers. This study reveals how correlated systems can reconcile the coexistence of different modes on interaction—by separating their action in momentum space, they allow their coexistence in real space.

INTRODUCTION

One of the earliest triumphs of the theory of many-body systems was the Kondo model of dilute magnetic impurities embedded in a metal (*1*). The theory describes the scattering of the conduction electrons by local moments via Kondo exchange, causing an increase in the resistance until, at some low temperature T_K, the conduction electrons become entangled with these moments, forming a neutral singlet with strongly suppressed scattering of the carriers. Doniach and others (*2*–*4*) suggested that this idea could be extended to some classes of lanthanide and actinide compounds that form lattices of local f moments, in which case, the lattice singlets themselves should conserve crystal momentum and form a heavy FERMI liquid at the Kondo coherence temperature. However, the Rudderman-Kittel-Kasuya-Yoshida (RKKY) interaction, which is closely related to Kondo exchange, can also favor the magnetic ordering of the magnetic ions, and so, the f electrons must choose between these two paths. In principle, magnetic ordering and Kondo entanglement should be mutually exclusive, but in general, signatures of both mechanisms are evident in most materials, as if the two states coexist. The semimetal CeSb is a case where these signatures appear to be coincident, raising the question of how the f moments decide on the most favorable channel of interaction (*5*–*7*). The debate turns on understanding the complex interplay between symmetry and exchange, highlighting the importance of symmetry-sensitive measurements of the interacting f electrons.

The high-temperature paramagnetic (PM) state of CeSb is characterized by an enhanced heat capacity with a Sommerfeld coefficient $\gamma \sim 450$ mJ/mol·K^2 and a huge resistivity (with residual of ~ 600 microhm·cm), as shown in Fig. 1 (A and B). As the temperature decreases, there is a slight upturn of the resistivity, consistent with Kondo scattering (*8*), preceding a precipitous drop in both the heat capacity and the resistivity of the system. This drop begins well above the magnetic transition occurring at T_N^0, which is the first of a cascade i of transitions with critical temperatures T_N^i. Each of these magnetic phases is composed of ferromagnetic (FM) and PM layers of Ce moments, stacked antiferromagnetically in the [001] crystallographic direction with a well-defined wave vector k. Each transition can be thought of as a precursor of the lowest temperature phase at T_N^f illustrated in Fig. 1C, known as type IA antiferromagnetic (AFM) (*9*). As temperature increases, the ith transition will gain a PM layer, reducing the translational symmetry. The onset of magnetic order only accelerates the suppression of the heat capacity and resistivity, settling on a low-temperature Sommerfeld coefficient of ~20 mJ/mol·K^2 and residual resistivity $\rho_0 \sim 2$ microhm·cm, both more than two orders of magnitude smaller than the values extrapolated from the high-temperature state.

The interplay of symmetry and exchange in CeSb

The signatures of magnetic order and Kondo-like behavior are essentially coincident; as the temperature is lowered, the first magnetic transition occurs at $T_N^0 = 16.5$K, which is preceded by a downturn in the resistivity and the release of ~0.65Rln2 magnetic entropy at $T_{\tilde{K}} \sim 16$K. The latter effects are signatures that resemble the properties of Kondo metals, but because Kondo interactions must be weak in CeSb, we use the notation $\tilde{K}$ to distinguish it from the Kondo coherence that appears in other systems. To qualify this, we compare the resistivity of CeSb to that of $CeCoIn_5$, an archetypical Kondo metal, which shows a much more marked Kondo upturn in the resistivity. Note that absolute values of the resistivities differ by one order of magnitude, which is reasonable given the carrier density is about 100 times smaller in CeSb, while its effective mass is only 10 times smaller (*10*–*12*).

The Kondo behavior in CeSb is weak because the itinerant carriers are few, consisting of small electron- and hole-like Fermi surfaces (see fig. S4). Since the Fermi momentum k_F is therefore small, FM correlations are favored by the RKKY interaction (*13*), consistent with the in-plane FM order. The unusual nature of the AFM transitions is more difficult to understand, but it is thought to arise out of the interplay of symmetry and exchange in the ground-state interactions. The f ground state has a Γ_7-type symmetry (*14*); as shown in Fig. 2C, spin-orbit (SO) coupling separates the f states into $^7/_2$ and $^5/_2$ multiplets,

[1]Advanced Light Source, Lawrence Berkeley Laboratory, Berkeley, CA 94720, USA. [2]Department of Physics, University of California, Berkeley, CA 94720, USA. [3]Materials Sciences Division, Lawrence Berkeley National Laboratory, Berkeley, CA 94720, USA. [4]Department of Chemistry and Division of Advanced Nuclear Engineering, POSTECH, Pohang 37673, Korea. [5]Department of Physics and Astronomy, Rice University, Houston, TX 77005, USA. [6]Department of Physics, Arizona State University, Tempe, AZ 85281, USA.
*Corresponding author. Email: analytis@berkeley.edu (J.G.A.); jddenlinger@lbl.gov (J.D.D.); jsyquf777@gmail.com (S.J.)

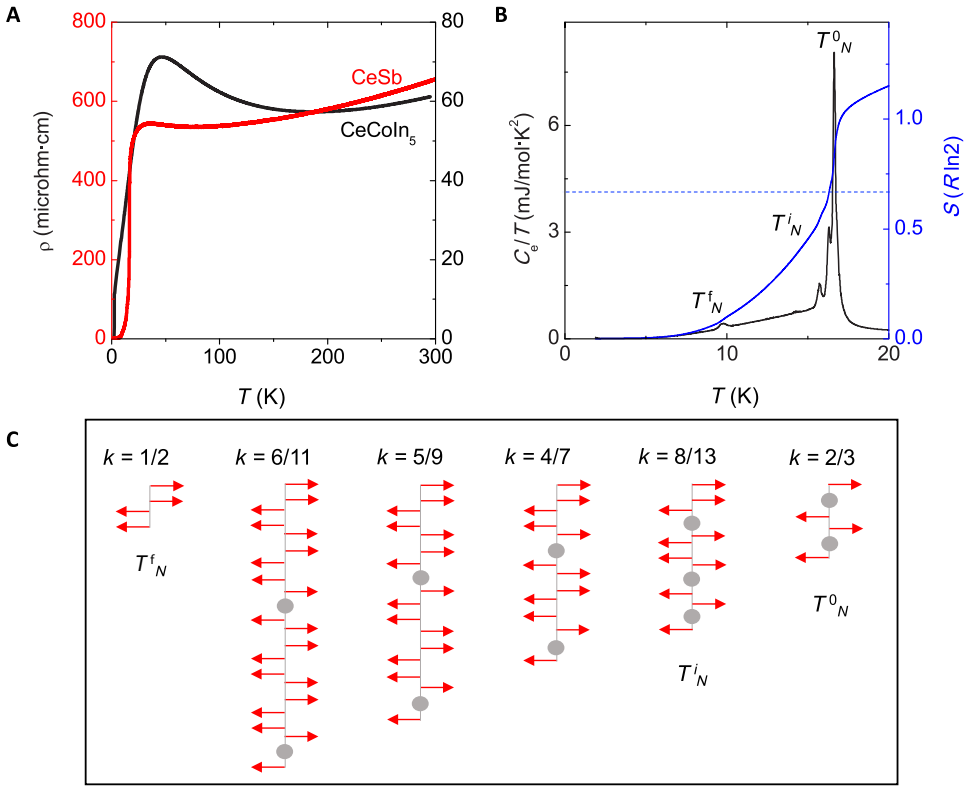

Fig. 1. Magnetic and Kondo-like behavior in CeSb. (**A**) Temperature dependence of the electrical resistivity for semimetal CeSb and typical Kondo system $CeCoIn_5$, coherence peak at T^* ~ 35 and 45 K, respectively signaling the presence of the Kondo scattering at high temperature for both compounds. Although the absolute residual resistivity of CeSb is much greater than that of $CeCoIn_5$ due to its semimetallic nature, the relative size of the resistivity upturn preceding T^* is significantly smaller. (**B**) Electronic specific heat (C_e; black line with left axis) shows several magnetic transitions, from the AFM/PM transition at T_N^0 = 17 K to the AFM/FM-phase transitions at T_N^f = 8 K. Entropy (S; blue line with right axis) has been estimated by integrating the electronic specific heat, suggesting that spin degrees of freedom are restored at $T_{\tilde{K}}$ ~ 16K. (**C**) Schematic of the magnetic structure at each transition T_i across the so-called Devil's staircase. Red arrows and gray circles present the direction of each FM and PM layers, respectively.

and the latter is split by the crystal electric field (CEF) into a Γ_8 quartet and a Γ_7 doublet. The hole-like Fermi pockets from the Sb band also have Γ_8 symmetry, which leads to a large interaction with the quartet. Kasuya and colleagues (*15*, *16*) have argued that, while Kondo exchange is important to understand the overall properties of CeSb, a critical mechanism behind the magnetic anisotropy of the ordered state is hybridization, which pulls down fΓ_8 states so that they mix with the ground state. Other authors have argued for non-Kondo exchange, mediated by both electrons and holes and independent of their symmetry (*5*, *6*), although p-f hybridization is still invoked to explain the appearance of PM layers (*7*). These latter proposals do not require an active Kondo interaction, leaving the observed Kondo signatures to be explained by some alternative mechanism. Both pictures require that the CEF is small, and this has been measured to be ~3 meV (*14*). Distinguishing these pictures and explaining the dichotomous properties of CeSb requires symmetry-resolved measurements of the interaction between the Ce f moments and the hole and electron Fermi pockets. To this end, we turn to angle-resolved photoemission spectroscopy (ARPES).

RESULTS

Recent ARPES studies on CeSb have largely focused on verifying whether the system contains a Weyl-like crossing at the X point of the Brillouin zone (BZ), ostensibly arising from a p-d band inversion (*17*–*19*), but only a few have addressed the question of the magnetism itself (*20*) (we comment on the possible presence of Weyl-like features in sections S2 and S3). The three-dimensional (3D) nature of the Fermi surface creates a number of complications in obtaining reliable data on CeSb: The probed region of the BZ depends strongly on the photon energy, bulk bands and surface projections of those bands must be carefully distinguished, and orbital selection rules couple some bands preferentially to a given photon polarization and energy (see section S1 for more details). Therefore, we perform our measurements at different polarizations, linear horizontal (LH) and linear vertical (LV) lights, and photon energies ranging between 30 and 158 eV to access the intrinsic bulk behavior. We focus on using photons that couple resonantly to the Ce 4d → 4f transition ($h\nu$ = 122 eV), which strongly enhances the contribution of the f states. This can be broadly thought of as orbital-specific ARPES, because it enhances the features related to the Ce f-state interaction across the magnetic transitions.

Figure 2A shows several prominent Ce 4f-related features in the angle-integrated density of states (DOSs), which can be distinguished by their absence in the off-resonance data. There is a strong feature at binding energy $E - E_F$ ~ 2.9 eV, corresponding to the f^0 final-state peak associated with the cost of removing one electron from the trivalent Ce ion ($4f^1 \rightarrow 4f^0$). In addition, there are two other features at

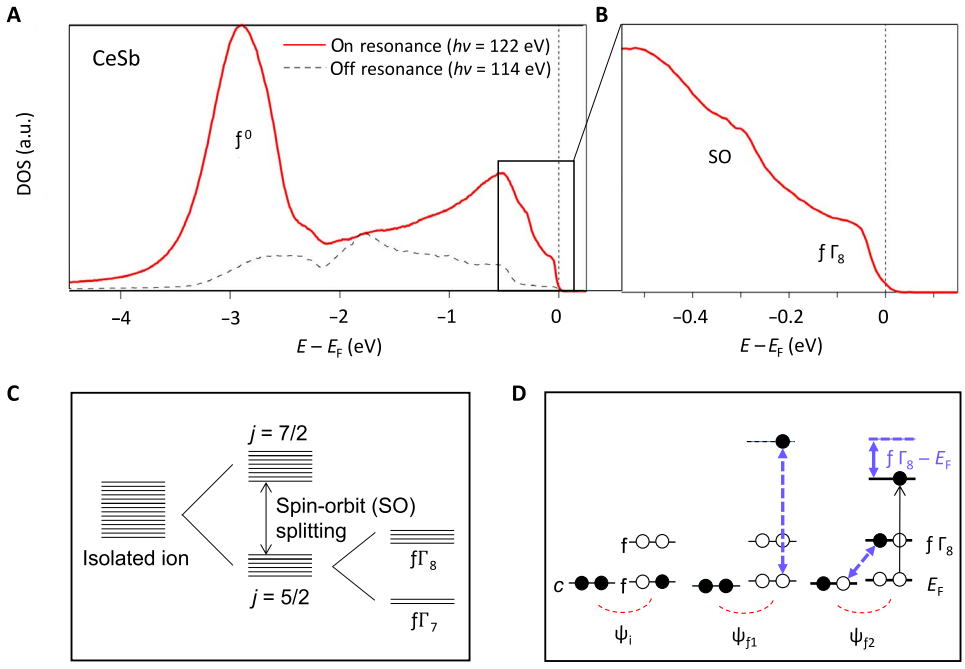

Fig. 2. CEF splitting. (**A** and **B**) The *k*-integrated f density of state (DOS) for on- and off-resonance ARPES data is displayed by red solid line and gray dashed line, respectively. Each f state is indicated by fΓ_8 CEF, SO side-band peak and the f^0 final-state peak in the range of binding energy ($E_B = E - E_F$) between 0.1 and −4 eV. a.u., arbitrary units. (**C**) Crystal field scheme of cubic CeSb. SO separates $J = {}^7/_2$ and ${}^5/_2$ multiplets, and the latter is split by CEF into doublet fΓ_7 and quartet fΓ_8 manifolds, with fΓ_7 forming the ground state. (**D**) Schematic of final-state shake-up transitions for Ce $4f^1$ including initial state hopping between the conduction electrons (*c*) and the f states. Excitation into fΓ_8 CEF (or $J = 7/2$ SO split) f states results in lowered photoelectron kinetic energies at the detector and the appearance of these f states below E_F.

$E - E_F \sim 300$ and ~ 50 meV. The former is consistent with the known SO splitting of the f states in Ce systems, suggesting that the latter corresponds to the CEF splitting of the ${}^5/_2$ sextet. These states are actually above E_F but can be observed in photoemission due to "final-state excitations," explained schematically in Fig. 2D (*21*). In essence, the energy of the electrons reaching the detector depends on the final state of the system after the electron is removed so that multi-electron excitations to intermediate states lead to lower kinetic energy photoelectrons. The result is that SO and CEF excited states appear at binding energies below E_F, mirroring their excitation energies above E_F (distinguished as Γ_8^* states). This observation alone indicates that Kondo-like many-body effects are present by the following argument; note that Ce^{3+} only has one electron f^1 so that the electrons excited to the intermediate states must therefore originate from the itinerant electrons or holes, although the photon is resonant to f states. Nevertheless, although this is consistent with a Kondo-like entanglement of local moments with itinerant carriers, there is no clear Kondo resonance observed near the Fermi energy, suggesting that the Kondo effect is highly suppressed. This suppression of the E_F Kondo resonance causes a "pseudogap-like" appearance in the f DOS consistent with single-impurity spectral function predictions for the narrow width and deep binding energy of the f^0 peak, as shown in section S1.

The $E - E_F$ of ~50-meV feature has never been reported before. Although it is an order of magnitude larger than the CEF splitting reported in earlier studies of CeSb (*9*, *22*), it is consistent with CEF splitting reported in other Ce^{3+} compounds (*23*) and also with known trends in rare-earth pnictides (*24*). The early neutron measurements of CeSb did not explore these large energy scales, and the 3-meV feature, which appears as a shoulder on a large elastic peak, may correspond to an additional splitting. Our results suggest that neutron studies should be revisited to explore higher energy scales in CeSb, especially since so much of the theory on these compounds hinges on the correct CEF splitting of the Γ_7 and Γ_8 manifolds of the f states.

In Fig. 3, we show the evolution of the band structure near the *X* point of the BZ. At the first transition T_N^0, the d bands suddenly split, with a gap Δ that grows only slightly as the system is further cooled. Below T_N^f, where all PM layers have been extinguished, the splitting is ~100 meV (see Fig. 3, B to D), indicating a substantial exchange coupling between the fΓ_7 ground-state moments and the Ce d electrons. A schematic of the Zeeman-like exchange splitting is shown in Fig. 3 (A and E). This suggests that the dominant effect on the band structure is the influence of the FM planes and not of the interlayer AFM order, which would tend to fold the zone. There is no evidence of hybridization between the f states and the d electrons, which might be expected if Kondo-like behavior was active. Rather, the behavior of the d electrons appears to be strongly exchange-coupled to the ordering of the fΓ_7 moments, consistent with non-Kondo magnetism (*5*–*7*).

However, the behavior of the Sb p bands at the Γ point of the BZ stands in stark contrast to that of the Ce d bands at the *X* point. Figure 4 illustrates the temperature dependence of the two hole-like bands as the temperature is lowered. At high temperatures $T > 20$ K, the band structure and Fermi surface appear very similar to the nonmagnetic analog of this material LaSb (see section S4), with two p bands crossing the Fermi energy. These form hole-like Fermi surfaces with no apparent f character. As the temperature is lowered, the bands appear to curve at points where they cross the f states, particularly the inner p band with the fΓ_8 electrons. This hybridization is consistent with the

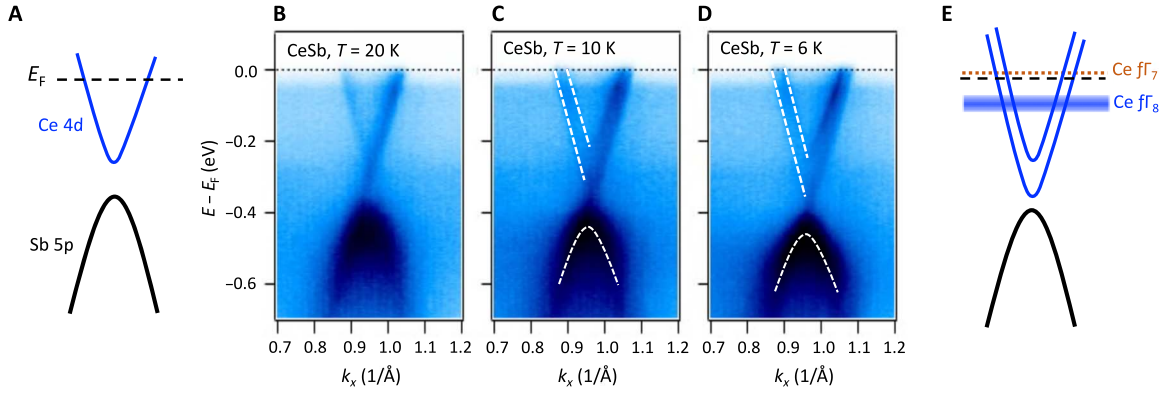

Fig. 3. Observation of magnetic exchange splitting at *X* point. Schematic of CeSb's band structure at *X*, (**A**) at $T > T_N^0$ (**E**) at $T < T_N^f$. (**B** to **D**) ARPES data taken at $h\nu$ = 88 eV near the *X* point for the selected temperatures (indicated at the top left). A clear signature of band splitting has been detected at T = 6 K owing to Zeeman-like exchange splitting, which disappears above T_N^0.

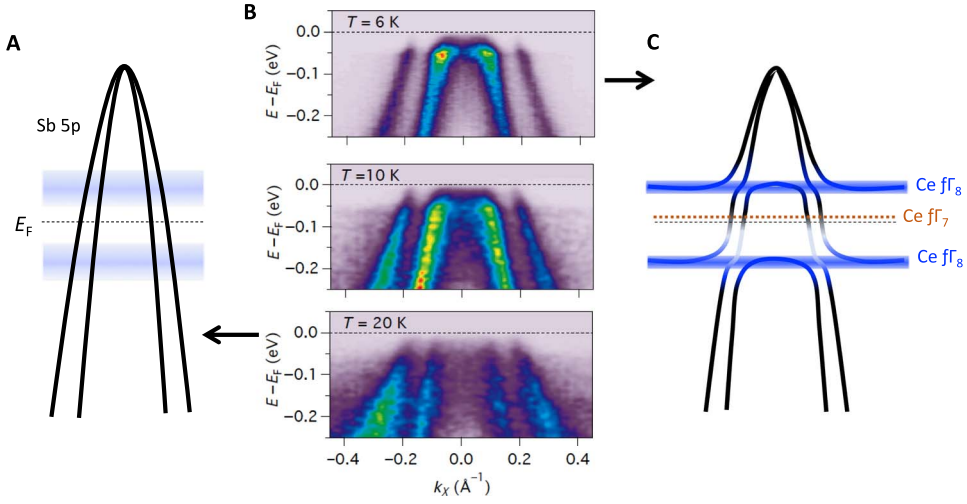

Fig. 4. Observation of p-f hybridization at the Γ point. Schematic of CeSb's band structure at Γ, (**A**) at $T > T^*$ and (**C**) at $T \ll T^*$. The schematic is a simplification and does not take into account orbital-dependent hybridization due to symmetry considerations nor the effect of final-state excitations. (**B**) Temperature dependence of the ARPES spectra showing strong evidence of p-f hybridization as the temperature is lowered. Note that a *k*-independent background has been subtracted from the spectral images (see section S5 and fig. S5). The on-resonance photon energy is 122 eV for k_Z at the high-symmetry Γ point of the bulk BZ (see fig. S2A).

symmetry-allowed interaction between the fΓ_8 states and the p bands with Γ_8 character. We do not see the exchange splitting of the kind observed at the *X* point. Since we resonantly enhance the signal from the f states, our data provide direct evidence that the dominant interaction between the f states and the p states is in the hybridization channel, as opposed to the exchange splitting seen at *X* point. We are thus able to make an important statement about the physics of CeSb; the interactions between the f electrons are strong with both p and d states, but they just choose different channels.

DISCUSSION

Understanding the complex magnetism of CeSb depends on a complete picture of how the f electrons interact with the electron and hole-like pockets (*7*, *16*, *25*). By symmetry, it is natural that the p bands have a strong interaction with the fΓ_8 states, just as we observe. However, given the large CEF indicated by our data, it seems less likely that this p-f hybridization will drive admixing of (part of) the fΓ_8 excited states with the fΓ_7 ground state, as required in some theoretical pictures of these materials (*16*). While there may be some magnetic interplay between the hybridized p electrons and the exchange splitting of the d electrons, the main result of this study is that the ground-state f moments interact in demonstrably different ways with the different carriers. The simultaneous activity of these interaction channels is quantum mechanically allowed because they occur in different parts of momentum space, painting an appealing picture for the CeSb's apparent dichotomous properties; coexisting signatures in the transport and magnetism that have previously been associated with Kondo-like screening and magnetic order could be an indirect manifestation of coexisting paths of interaction.

A Kondo resonance peak at E_F is, however, not evident in the spectroscopy (Fig. 2A). This suggests that Kondo-like exchange must be weak but not necessarily nonexistent. The presence of these interactions may be indirectly evident by the presence of final-state effects that allow the observation of CEF and SO excited states, as described above. More interesting are the apparent momentum-dependent interactions, whose mechanism may be analogous to processes in FM-Kondo materials, that have only recently been understood (*26*–*30*).

In these materials, the Kondo interactions are spin selective, allowing FM to coexist with partial Kondo screening. In CeSb, the interactions are orbitally selective, weaving FM layers with PM layers and magnetic order with partial Kondo screening.

Our observations in CeSb suggest an interesting paradigm for understanding the coexistent signatures of distinct many-body phenomena widely observed in correlated electron materials. A persistent question in the physics of heavy fermion materials has been why some itinerant quasiparticles are more susceptible to forming a Kondo coherence than others, which is evident in the coexistence of both heavy and light bands in many systems (*31*). Although the Kondo signatures of CeSb are extremely weak, the material, nevertheless, provides a clue as to how this can occur; f electrons can interact in different channels, depending on the orbital symmetry of the itinerant states themselves. The dichotomous nature of CeSb, marked by the coexistence in real space of different many-body phenomena, is allowed by the separation of different channels of interaction in momentum space.

MATERIALS AND METHODS

Single crystals of CeSb were synthesized using tin flux. Cerium (99.8%), antimony (99.9999%), and tin (99.999%) (all from Alfa Aesar) were added to an alumina crucible in a molar ratio of 1:1:20. The crucible was sealed in an evacuated quartz ampule before being heated over 8 hours at 1150°C, where it dwelled for 24 hours. Next, the ampule was cooled at 800°C over 24 hours, and then, it was centrifuged to remove excess tin. This procedure yielded 5- to 10-mm single crystals.

Temperature-dependent ARPES measurements were performed at the MERLIN Beamline 4.0.3 of the Advanced Light Source using both LH and LV polarizations from an elliptically polarized undulator. A Scienta R8000 electron spectrometer with 2D parallel detection of electron kinetic energy and angle in combination with a six-axis helium cryostat goniometer with 6 K of base temperature and $<5 \times 10^{-11}$ torr of base pressure was used. Total energy resolution of approximately 15 meV was used for measurements at $h\nu = 122$ eV corresponding to the Ce 4d-4f resonant enhancement of the f photoionization cross section.

SUPPLEMENTARY MATERIALS

Supplementary material for this article is available at http://advances.sciencemag.org/cgi/content/full/5/3/eaat7158/DC1

Section S1. Single impurity Ce 4f spectral weight
Section S2. ARPES data on LaSb
Section S3. Possible Weyl points within the fully ordered state
Section S4. Comparison of Fermi surface for CeSb and LaSb
Section S5. Background subtraction of the ARPES spectra at the Γ point
Fig. S1. Single-impurity Ce 4f spectral weight.
Fig. S2. Energy band dispersion at different photon energies and light polarizations.
Fig. S3. ARPES data on LaSb.
Fig. S4. Fermi surface map for CeSb and LaSb at $h\nu$ = 122 and 88 eV, respectively.
Fig. S5. Background subtraction of the ARPES spectra at the Γ point.
References (*32*, *33*)

REFERENCES AND NOTES

1. J. Kondo, Resistivity minimum in dilute magnetic alloys. *Prog. Theor. Phys.* **32**, 37–49 (1964).
2. R. Jullien, J. Fields, S. Doniach, Kondo lattice: Real-space renomalization-group approach. *Phys. Rev. Lett.* **38**, 1500–1503 (1977).
3. N. F. Mott, Rare-earth compounds with mixed valencies. *Philos. Mag.* **30**, 403–416 (1974).
4. S. Doniach, Kondo lattice and weak antiferromagnetism. *Physica B* **91**, 231–234 (1977).
5. B. Coqblin, J. R. Schrieffer, Exchange interaction in alloys with cerium impurities. *Phys. Rev.* **185**, 847–853 (1969).
6. B. R. Cooper, Contrasting behavior of light rare earth and actinide intermetallics. *J. Magn. Magn. Mater.* **29**, 230–240 (1982).
7. N. Kioussis, B. R. Cooper, A. Banerjea, Mechanism for the occurrence of paramagnetic planes within magnetically ordered cerium systems. *Phys. Rev. B* **38**, 9132–9144 (1998).
8. C. Guo, C. Cao, M. Smidman, F. Wu, Y. Zhang, F. Steglich, F.-C. Zhang, H. Yuan, Possible Weyl fermions in the magnetic Kondo system CeSb. *NPJ Quantum Mater.* **2**, 39 (2017).
9. J. Rossat-Mignod, P. Burlet, J. Villain, H. Bartholin, W. Tcheng-Si, D. Florence, O. Vogt, Phase diagram and magnetic structures of CeSb. *Phys. Rev. B* **16**, 440–461 (1977).
10. L. Ye, T. Suzuki, C. R. Wicker, J. G. Checkelsky, Extreme magnetoresistance in magnetic rare earth monopnictides. arXiv:1704.04226v1 [cond-mat.mtrl-sci] (13 April 2017).
11. M. F. Hundley, A. Malinowski, P. G. Pagliuso, J. L. Sarrao, J. D. Thompson, Anomalous *f*-electron Hall effect in the heavy-fermion system $CeTIn_5$ (T = Co, Ir, or Rh). *Phys. Rev. B* **70**, 035113 (2004).
12. T. A. Wiener, P. C. Canfield, Magnetic phase diagram of flux-grown single crystals of CeSb. *J. Alloys Compd.* **303–304**, 505–508 (2000).
13. K. Yamamoto, K. Ueda, Ground state and magnetization process of the one-dimensional Kondo lattice. *J. Phys. Soc. Jpn.* **59**, 3284–3288 (1990).
14. H. Heer, A. Furrer, W. Halg, O. Vogt, Neutron spectroscopy in the cerium monopnictides. *J. Phys. C Solid State Phys.* **12**, 5207–5220 (1979).
15. M. Kasaya, F. Iga, K. Negishi, S. Nakai, T. Kasuya, A new and typical valence fluctuating system, YbB_12. *J. Magn. Magn. Mater.* **31–34**, 437–438 (1983).
16. H. Takahashi, T. Kasuya, Anisotropic p-f mixing mechanism explaining anomalous magnetic properties in Ce monopnictides. V. Various ordered states and phase diagrams. *J. Phys. C Solid State Phys.* **18**, 2745–2754 (1985).
17. N. Alidoust, A. Alexandradinata, S.-Y. Xu, I. Belopolski, S. K. Kushwaha, M. Zeng, M. Neupane, G. Bian, C. Liu, D. S. Sanchez, P. P. Shibayev, H. Zheng, L. Fu, A. Bansil, H. Lin, R. J. Cava, M. Zahid Hasan, A new form of (unexpected) Dirac fermions in the strongly-correlated cerium monopnictides. arXiv:1604.08571v1 [cond-mat.str-el] (28 April 2016).
18. Y. Wu, Y. Lee, T. Kong, D. Mou, R. Jiang, L. Huang, S. L. Bud'ko, P. C. Canfield, A. Kaminski, Electronic structure of RSb (R = Y, Ce, Gd, Dy, Ho, Tm, Lu) studied by angle-resolved photoemission spectroscopy. arXiv:1704.06237v1 [cond-mat.mtrl-sci] (20 April 2017).
19. H. Oinuma, S. Souma, D. Takane, T. Nakamura, K. Nakayama, T. Mitsuhashi, K. Horiba, H. Kumigashira, M. Yoshida, A. Ochiai, T. Takahashi, T. Sato, Three-dimensional band structure of LaSb and CeSb: Absence of band inversion. arXiv:1707.05100v1 [cond-mat.mtrl-sci] (17 July 2017).
20. A. Takayama, S. Souma, T. Sato, T. Arakane, T. Takahashi, Magnetic phase transition of CeSb studied by low-energy angle-resolved photoemission spectroscopy. *J. Phys. Soc. Jpn.* **78**, 073702 (2009).
21. S. Hüfner, *Photoelectron Spectroscopy* (Springer, 1995).
22. J. Rossat-Mignod, J. M. Effantin, P. Burlet, T. Chattopadhyay, L. P. Regnault, H. Bartholin, C. Vettier, O. Vogt, D. Ravot, J. C. Achard, Neutron and magnetization studies of CeSb and $CeSb_{1-x}Te_x$ solid solutions. *J. Magn. Magn. Mater.* **52**, 111–121 (1985).
23. A. Koitzsch, N. Heming, M. Knupfer, B. Büchner, P. Y. Portnichenko, A. V. Dukhnenko, N. Y. Shitsevalova, V. B. Filipov, L. L. Lev, V. N. Strocov, J. Ollivier, D. S. Inosov, Nesting-driven multipolar order in CeB_6 from photoemission tomography. *Nat. Commun.* **7**, 10876 (2016).
24. R. J. Birgeneau, E. Bucher, J. P. Maita, L. Passell, K. C. Turberfield, Crystal fields and the effective-point-charge model in the rare-earth pnictides. *Phys. Rev. B* **8**, 5345–5347 (1973).
25. T. Kasuya, Y. Hasa, Y. S. Kwon, T. Suzuki, Physics in low carrier strong correlation systems. *Physica B* **186–188**, 9–15 (1993).
26. Th. Pruschke, R. Bulla, M. Jarrell, Low-energy scale of the periodic Anderson model. *Phys. Rev. B* **61**, 12799–12809 (2000).
27. L. Yu, G.-M. Zhang, L. Yu, Weak ferromagnetism with the Kondo screening effect in the Kondo lattice systems. *Phys. Rev. B* **87**, 134409 (2013).
28. R. Peters, N. Kawakami, T. Pruschke, Spin-selective Kondo insulator: Cooperation of ferromagnetism and the Kondo effect. *Phys. Rev. Lett.* **108**, 086402 (2012).
29. D. Golež, R. Žitko, Lifshitz phase transitions in the ferromagnetic regime of the Kondo lattice model. *Phys. Rev. B* **88**, 054431 (2013).
30. S. J. Yamamoto, Q. Si, Metallic ferromagnetism in the Kondo lattice. *Proc. Natl. Acad. Sci. U.S.A.* **107**, 15704–15707 (2010).
31. R. Movshovich, T. Graf, D. Mandrus, J. D. Thompson, J. L. Smith, Z. Fisk, Superconductivity in heavy-fermion $CeRh_2Si_2$. *Phys. Rev. B* **53**, 8241–8244 (1996).
32. N. E. Bickers, Review of techniques in the large-*N* expansion for dilute magnetic alloys. *Rev. Mod. Phys.* **59**, 845–939 (1987).
33. O. Sakai, Y. Shimizu, DMFT band calculation for Ce compounds. *J. Magn. Magn. Mater.* **310**, 374–376 (2007).

Acknowledgments: We would like to thank P. Canfield, J. Checkelsky, and P. Coleman for helpful discussions. **Funding:** Synthesis and thermodynamic properties characterization

by R.K. and J.G.A. was supported by the NSF under grant no. 1607753. S.J., R.K., and J.G.A. acknowledge support from the Gordon and Betty Moore Foundation's EPiQS Initiative through grant no. GBMF4374. This research used resources of the Advanced Light Source, which is a DOE Office of Science User Facility under contract no. DE-AC02-05-CH11231. R.K. acknowledges support by the NSF Graduate Research Fellowship, grant no. DGE-1106400. J.H.S. and J.-S.H. were supported by the National Research Foundation of Korea (NRF) grant funded by the Korea government (MSIP; no. 2015R1A2A1A15051540). The work at Rice University is supported by the NSF grant no. DMR-1611392, the Robert A. Welch Foundation grant no. C-1411, the ARO grant no. W911NF-14-1-0525, and a QuantEmX grant from ICAM and the Gordon and Betty Moore Foundation through grant no. GBMF5305. Q.S. acknowledges the hospitality of University of California at Berkeley. **Author contributions:** S.J., J.D.D., and J.G.A. conceived the experiment. R.K., C.J., and S.D. synthesized single crystals and performed the transport measurement. J.S.H. and J.H.S. provided theoretical support to understand the effect of correlations on the band structure. Q.S. and O.E. discussed the experimental results and provided theoretical analysis. S.J. and J.D.D. conducted ARPES measurements. All authors contributed to the writing of the manuscript. **Competing interests:** The authors declare that they have no competing interests. **Data and materials availability:** All data needed to evaluate the conclusions in the paper are present in the paper and/or the Supplementary Materials. Additional data related to this paper may be requested from the authors.

Submitted 4 April 2018
Accepted 22 January 2019
Published 1 March 2019
10.1126/sciadv.aat7158

Citation: S. Jang, R. Kealhofer, C. John, S. Doyle, J.-S. Hong, J. H. Shim, Q. Si, O. Erten, J. D. Denlinger, J. G. Analytis, Direct visualization of coexisting channels of interaction in CeSb. *Sci. Adv.* **5**, eaat7158 (2019).